Waste Cleaning Waste: Combining Alginate with Biowaste-Derived Substances in Hydrogels and Films for Water Clean-up

Maria Laura Tummino,[a]* Roberto Nisticò,[b] Chiara Riedo,[a] Debora Fabbri,[a] Marta Cerruti,[c] and Giuliana Magnacca,[a,d]*

[a] Dr. M. L. Tummino, Dr. C. Riedo, Prof. D. Fabbri, Prof. G. Magnacca
Department of Chemistry
Università degli Studi di Torino
Via P. Giuria 7, 10125 Torino, Italy
Email: marialaura.tummino@unito.it
chiara.riedo@unito.it
debora.fabbri@unito.it
giuliana.magnacca@unito.it

M. L. Tummino's present address:

[b] Dr. R. Nisticò
Independent Researcher
via Borgomasino 39, 10149 Torino, Italy
Email: roberto.nistico0404@gmail.com

[c] Prof. M. Cerruti
Department of Mining and Materials Engineering
McGill University
Montreal, QC H3A 2B2, Canada
Email: marta.cerruti@mcgill.ca

[d] Prof. G. Magnacca
NIS centre
Via P. Giuria 7, 10125 Torino, Italy
Email: giuliana.magnacca@unito.it

Supporting information for this article is given via a link at the end of the document.((Please delete this text if not appropriate))

Abstract: Biowaste-derived substances isolated from green compost (BBS-GC) are environmental-friendly reactants similar to humic substances, which bring multiple functionalities, suitable to adsorb different kinds of pollutants in wastewater. Here we propose sodium alginate (derived from brown algae) crosslinked with both Ca^{2+} ions and BBS-GC in the form hydrogels and dried films as green, easy-to-form and handleable materials for tertiary water treatments. Our results show that both hydrogels and films are mechanically stable and can effectively remove differently charged dyes through an adsorption mechanism describable by the Freundlich model. BBS-GC-containing gels always performed better than samples prepared without BBS-GC, revealing that such unconventional materials can integrate waste valorization and water decontamination, potentially providing social and environmental benefits.

Introduction

Access to safe water is a concern for a large part of the global population and both climate change and the increasing pollution are exacerbating the problem. [1] Traditional solutions to purify water include biodegradation, adsorption, filtration, flocculation, membrane separations and ion exchange resins. [2, 3] Tertiary treatments performed at the final stage of water depuration more and more incorporate innovative materials and methods to bring the effluent quality to the desired level of purity before water is reused, recycled or discharged into the environment. [4] In particular, new kinds of not commonly monitored refractory pollutants (Contaminants of Emerging Concern, CECs) detected at trace/sub-trace level in water bodies can bypass the depuration stages of traditional wastewater plants, thus need advanced strategies for their removal. [3]

Although adsorption represents a classical method, it is still one of the most studied approach for water depuration, as confirmed by the huge amount of published papers on such theme (more than 21000 in the last five years, according to Scopus, searching for "pollutant AND adsorption"). The main reasons for this "success" are the easiness and cost convenience of the process. [5] Additionally, its versatility makes this method suitable for water purification from recalcitrant compounds. [5] Indeed, this process requires that species soluble in a medium are captured by active sites present at the adsorbent surface. The adsorption effectiveness is influenced by the electronic structure of adsorbent and adsorbate, [6] the interactions among their respective functional groups, [7] and the adsorbent surface morphology [7]. Among adsorbents, one of the oldest and most commonly used material is activated carbon [8] but also mineral-based compounds, such as silica gels, activated alumina, zeolites, clay minerals, have been widely studied. [9] Even more complex efforts have been made to develop innovative and effective adsorbing materials, often resorting to elaborate synthesis routes and/or non-sustainable reactants which makes unfavorable the up-scaling of the processes. [10-16] In this perspective, the simplicity of the materials' preparation and the use of bio-based recovered chemicals are aspects that should prevail over the pursuing of elaborated, complex, even if very active materials. In fact, in the last years, the scientific community has started investigating refuses as adsorbing agents, i.e. supported humic acids, [17] polysaccharides (as chitosan, alginate, starch, cellulose) and many kinds of industrial, agricultural or domestic by-products [18] such as shells of dried fruit and seeds, different wood species, sawdust, fruit peels,

lignin discharged from paper mills and microbial biomasses. [18, 19] The utilization of such raw materials can lighten the social burdens related to waste accumulation, as wastes can become new resources with no added production costs.

Among these materials, alginates are particularly promising: isolated from the cell walls of various species of brown algae, [20] they are low-cost, biocompatible and biodegradable. Due to this, alginates have been tested in many fields, [21, 22] including biomedical applications, [23] food technology, [24] energy, [25] cultural heritage preservation [26] and environmental remediation. [27]

Alginates are linear copolymers made by (1-4)-linked residues of β-D-mannuronic acid and α-L-guluronic acid units (Figure S1A). They can be crosslinked in the form of hydrogels by multivalent ions or other molecules with chemical functionalities that can react with alginate carboxylate groups, forming stable and non-soluble 3D networks. [28] Alginate hydrogels have already shown adsorbing capacity towards dyes, [29] metals, [27] inorganic species [30] and polycyclic aromatic hydrocarbons traces, [31] thanks to the free carboxylate and -OH groups that can act as chelation/coordination sites.

The adsorption saturation limit of alginate gels can be increased by increasing the space within the alginate chains to favor adsorbate molecules diffusion within the network with consequent increase of interactions. [22] Thus, additional substances with a suitable structure and bringing reactive functional groups can be inserted in the alginate framework during the gelification step to produce materials with enhanced adsorbing capacity. [32]

In this paper we tested the possibility of increasing the adsorption capacity of easy-to-form alginate gels using a biowaste-derived compound, i.e. bio-based substances extracted from several month-composted green waste (BBS-GC). BBS-GC are water-soluble macromolecules with a complex lignin-derived structure, similar to humic-fulvic acids, containing acid and basic functional groups bonded to aromatic and aliphatic chains (Figure S1B), and an inorganic residue derived from the acid/base separation procedure carried out on the starting compost: [33] BBS-GC composition is reported in Table S1. The many functional groups present on BBS-GC make this compound an excellent candidate for removal of aqueous contaminants: silica-grafted BBS-GC have been used to remove orange II, rhodamine B and inorganic ions, [3] whereas BBS-GC supported on alumina were used to remove crystal violet, carbamazepine and atenolol, demonstrating these macromolecules possess an interesting affinity to CECs, useful for their removal. [34] In addition to this point, BBS-GC can be light-activated (they were used as photosensitizers in several studies) [35] and could be used, at least in principle, in Advanced Oxidation Processes to achieve the degradation of the adsorbed pollutants induced by UV-Vis irradiation. Furthermore, it is important to highlight both the environmental and economic sustainability of including BBS-GC within a material formulation as a reactant. In the following, a cost analysis of the BBS-GC/Ca/alginate gels is reported. According to the IMR's Quarterly Review of Food Hydrocolloids, the market cost for food-grade alginate salts is estimated being in the 7.5-8.5 €/kg range, in 2002. [36] Additionally, the most used ionic cross-linking agent (which has been exploited also in the present study) is calcium cation (Ca^{2+}), typically obtained from calcium chloride ($CaCl_2$), calcium carbonate ($CaCO_3$) and calcium sulfate ($CaSO_4$), the latter two showing a lower solubility in aqueous environment (and, consequently, exerting a further control of the gelation process). [37] The costs of calcium chloride is estimated to be *ca.* 0.25 €/L or more (depending on the purity degree, and the sources adopted). [38] However, Ca-salts can be isolated also from marine biomasses (e.g., from the demineralization step of crustaceans' shells during the chemical processing of chitin), thus reducing dramatically the costs. [39] On the other hand, BBS-GC are biopolymers isolated from anthropogenic biowastes, whose extraction cost has been estimated being *ca.* 0.1-0.5 €/kg, depending on the waste source (see ref.[40] and references therein). Therefore, the higher the partial replacement of alginate with BBS-GC, the higher the economic advantages. Additionally, the Alg-Ca-BBS system here proposed is completely bio-based and environmentally sustainable as all components are (or might be) derivable from biomasses and are biodegradable and with no impact on the environment. At last, the use of BBS-GC in high technological applications, like the one presented in this paper, allows promoting the separate collection of biological residues, as already performed by several municipalities around the world.

We recently suggested chitosan-alginate-BBS-GC gels for dye adsorption; [22] the results obtained were promising, however some issues related to the preparation step were observed. Na-alginate and chitosan are soluble in water at different pH values; additionally, both the biopolymers originate viscous solutions and this can be a disadvantage for the mixture homogenization. When alginate and chitosan are mixed, their chains have to slide on each other to allow the interaction of chitosan amino groups with alginate carboxylic groups for the formation of the 3D polyelectrolyte complex (PEC). [22, 41]

To overcome the issues correlated with the engagement of multiple biopolymers, we designed a simpler system: here we adopted BBS-GC as a co-crosslinker along with Ca^{2+} ions to prepare alginate hydrogels. Indeed, calcium ions (bringing two positive charges) are able to create anchoring points for two carboxylic groups belonging to alginate chains and/or to BBS-GC molecules, possibly enhancing the stability of the gel. [41] We tested the ability of such BBS-GC-Ca-crosslinked gels to capture dyes that are typical pollutants identifiable downstream of textile and paper industries: [42-44] orange II (OII, negatively charged), rhodamine B (RH, zwitterionic) and crystal violet (CV, positively charged), whose molecular structures are reported in Figure S2. We prepared and tested also dried films (xerogels) [45] with the same composition, since their storage is simpler as they do not require a humid environment to keep the hydration state. At the end, we realized a proof of concept that BBS-GC can be used efficiently in alginate-based gel formulation for environmental applications, whereas the optimization of the material will remain object of future studies.

Therefore, the novelty of this work can be summarized in three points: (i) the tuning of well-known alginate gel adsorbent by a green additive rich of active chemical functionalities, enhancing its performances (also in a perspective of CECs' removal); (ii) the use of renewable substances, in particular biowaste-derived ones (that can bring about environmental hazards, if not properly disposed), instead of complexly synthesized materials, in a view of limited costs and circular economy; (iii) the improvement of the easiness of the system preparation and handleable use, which are important goals for innovative upgradable depuration methods, although based on traditional techniques; (iv) in a

future perspective, the presence of BBS-GC in the network could allow the decomposition of the adsorbed contaminants by light activation.

Results and Discussion

Gel preparation and physicochemical characterization

Following a previously reported procedure, [22] we developed different formulations of hydrogels and films (samples without BBS-GC were used as controls): Table 1 lists the names that we will use to identify the samples throughout this work. Figure 1A summarizes the steps of sample preparation with the digital pictures of both hydrogels and dried films. BBS-GC-containing samples are characterized by a brown color.

Table 1. Sample names used in this work for each formulation

Sample	Composition	Hydration state
Alg-Ca(H)	alginate: $CaCl_2$ = 2:1	Hydrated gel
Alg-Ca(F)	alginate: $CaCl_2$ = 2:1	Dried film
Alg-Ca-BBS(H)	alginate: $CaCl_2$: BBS = 2:1:1	Hydrated gel
Alg-Ca-BBS(F)	alginate: $CaCl_2$: BBS = 2:1:1	Dried film

After the crosslinking, we checked the stability of Alg-Ca and Alg-Ca-BBS gels and removed excess crosslinkers through several rinsing cycles. Figure 1B shows the desalination results in terms of chloride release, obtained for Alg-Ca-BBS(H). All the hydrogels behaved similarly: after 10 rinsing cycles (approximately 100 minutes), the Cl^- concentration was below 1 mg L^{-1}. The release of BBS-GC, evaluated on the supernatant after 10 washing cycles by UV-vis spectroscopy (Figure 1C), amounted to approximately 10% of the weight of BBS-GC employed for the gel preparation.

We evaluated the swelling of the dried films to ascertain that the 3D-network, when hydrated, is insoluble and analyze their ability to absorb water [46] (see Experimental Section for calculation). Figure 1D shows the swelling ratios as a function of time: BBS-GC limit the film rehydration, probably because their hydrophobic moieties hinder interaction with water, whereas other polar functionalities can be engaged with Ca^{2+} ions and polar groups of alginate, acting as further crosslinking points. These swelling values are noticeably lower than those obtained from the previously investigated alginate-chitosan-BBS-GC hydrogels, [22] since chitosan is well-known to be hygroscopic. [47]

We determined the amount of water entrapped in the hydrogels Alg-Ca(H) and Alg-Ca-BBS(H) by performing thermogravimetric analysis (TGA) in nitrogen in the range 30-200°C (Figure S3). The water content for both hydrogels was comprised between 96 and 97%. The weight loss associated with water occurred steadily till 150°C, suggesting that water molecules experienced a variety of interactions (hydrogen bonds) among them, with Ca^{2+} cations and with functional groups of alginate and BBB-GC, when present. [48]

We employed TGA under N_2 atmosphere to evaluate the thermal stability of dried films Alg-Ca(F) and Alg-Ca-BBS(F), compared with that of bare BBS-GC and sodium alginate (Figure 2A). BBS-GC films showed three main weight losses: a first contribution at approximately 100°C due to water evaporation, a second extensive loss in the 200-600°C temperature range corresponding to the degradation of the organic matrix and a third contribution at T > 600°C attributable to its progressive carbonization. The residue at 800°C of 41±2 wt.% was due to both carbonaceous moieties (derived from the conversion of BBS-GC to-char) and inorganic ashes already present in the pristine material (see Table S1). Weight losses of Na alginate occurred first at around 100°C due to the dehydration step, then from 200°C corresponding to the carbonization of the alginate chains and the formation of Na_2CO_3, [22] whereas the last phenomenon at temperatures higher than 700°C was due to the decomposition of sodium carbonate. [49] The final residue of sodium alginate at 800°C was estimated as 11±1 wt.%.

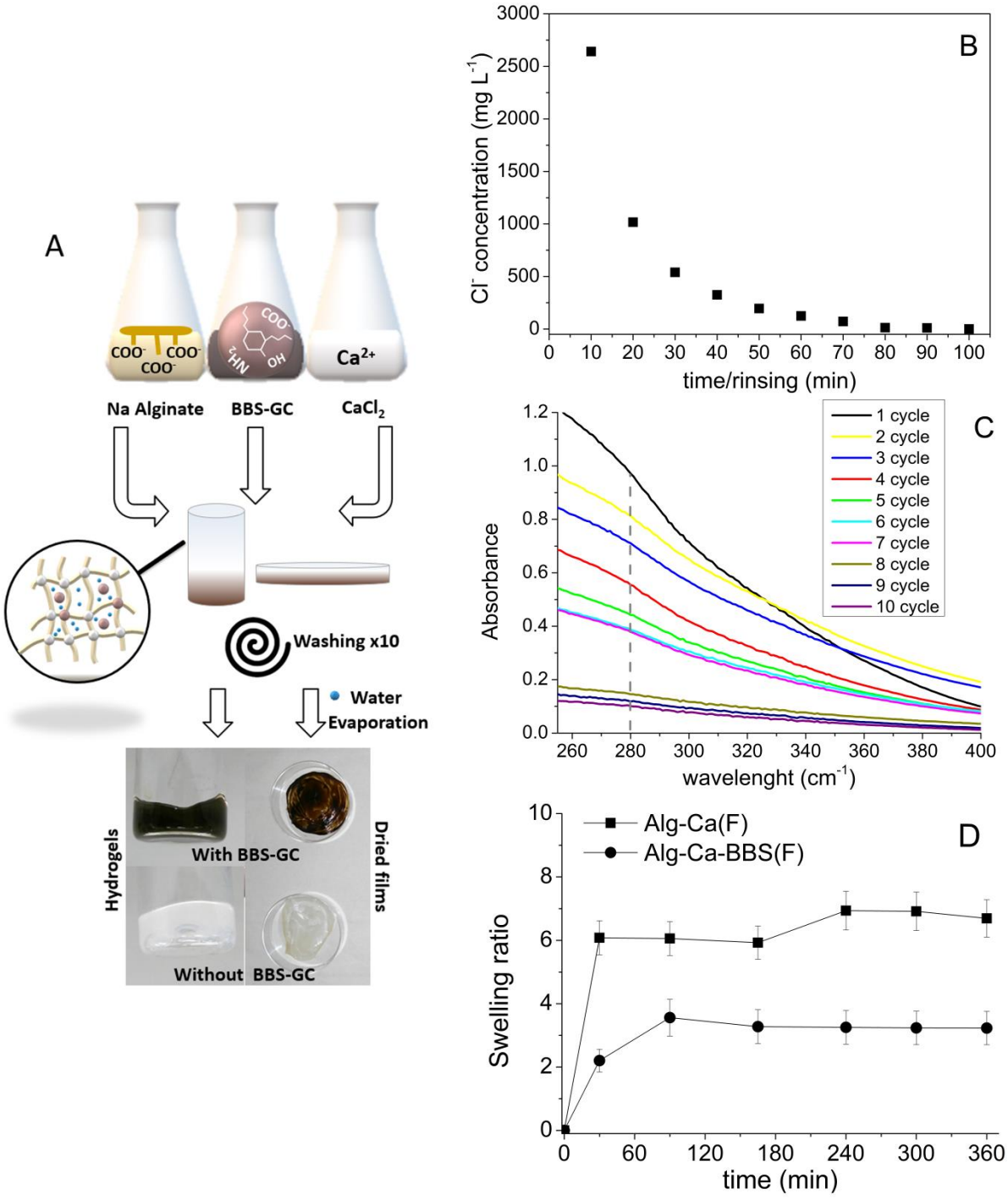

Figure 1. (A) Scheme of gel samples production; (B) chloride removal and (C) spectra of released BBS-GC as a function of the time (10 min/rinsing cycle) during the cleaning procedure for Alg-Ca-BBS(H); (D) time dependence of swelling ratios for dried films.

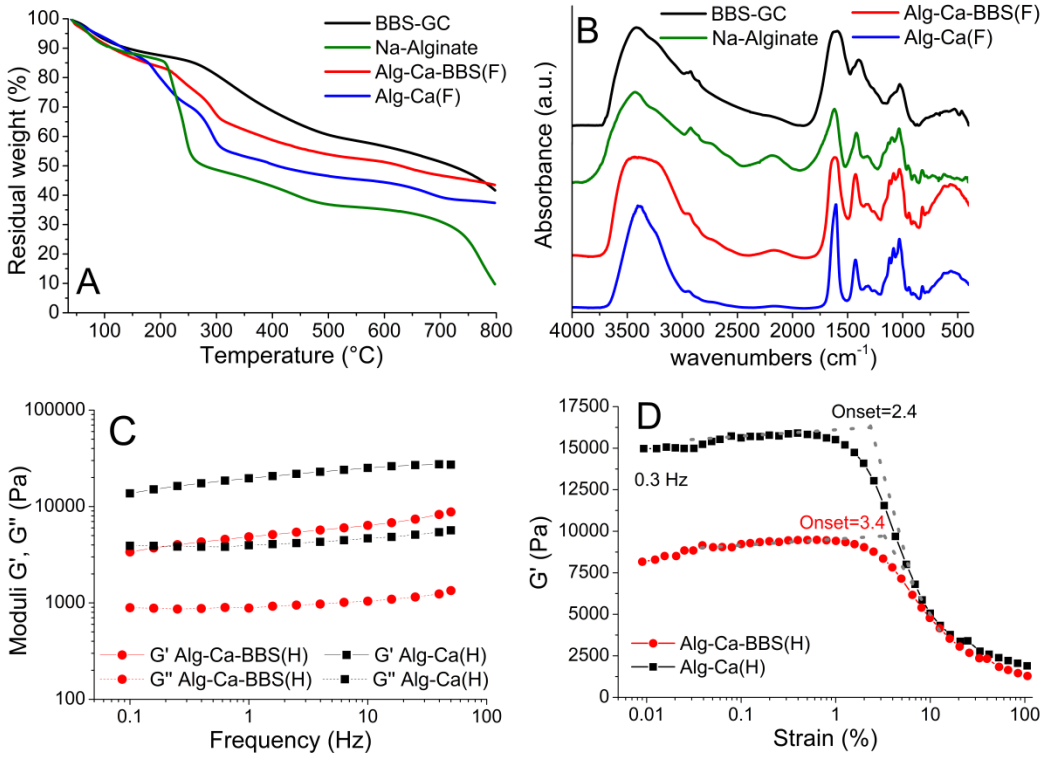

Figure 2. (A) TGA profiles measured in N_2 and (B) FT-IR spectra of BBS-GC, sodium alginate, Alg-Ca(F) and Alg-Ca-BBS(F); (C) frequency sweeps for the storage G' and loss G" moduli for Alg-Ca-BBS(H) and Alg-Ca(H); (D) strain sweep at fixed frequency of 0.3 Hz for Alg-Ca-BBS(H) and Alg-Ca(H).

Both films Alg-Ca(F) and Alg-Ca-BBS(F) showed similar thermal profiles with a preliminary dehydration step at about 100°C, followed by a multistep degradation profile starting from 200°C due to the progressive conversion of alginate and, if present, BBS-GC to char. In the presence of Ca^{2+} the gels started decomposing at lower temperature than sodium alginate, but the decomposition occurred slowly, indicating a good thermal stability of the 3D network in agreement with the literature. [50] BBS-GC contain inorganic components which, together with calcium, contributed to the formation of a final residue at 800°C of 39±5 wt.% for Alg-Ca-BBS(F) and 33±4 wt.% for Alg-Ca(F).

Figure 2B reports the Fourier transform infrared (FT-IR) spectra of the dried films together with those of bare components BBS-GC and Na-alginate. The BBS-GC IR spectrum (black curve) presents signals around 3400 cm^{-1} due to v(O-H) and v(N-H) modes, weak signals below 3000 cm^{-1} due to v(CH) and an intense signal in the 1700-1500 cm^{-1} range due to carboxylate and amide groups v_s(C=O), whereas signals at 1420 cm^{-1} are attributable to δ(C-H) and/or v_{as}(-OC=O) modes of carboxylate groups. Lastly, the signal at 1035 cm^{-1} is due to v(C-O-C) and/or δ(=C-H). [3] Analogous absorptions were registered also in the case of alginate spectrum as it has functional groups similar to BBS-GC. The IR main signals for neat alginate (green curve) are: a strong and broad band due to the v(O-H) of OH groups and H_2O molecules interacting via H-bonding centered at 3440 cm^{-1}, superimposed bands at 2920-2850 cm^{-1} ascribable to v(C-H) modes, two absorption bands centered at 1620 and 1460 cm^{-1} ascribable to the v_{as}(-OC=O) and v_s(-OC=O) modes respectively, as well as bands in the 1110-940 cm^{-1} range assigned to polysaccharide pyranosyl ring v(C-O) and v(C-O-C) vibrational modes. [51, 52] The large and non-well defined signal above 2000 cm^{-1} is due to some moisture contained in the powder (combination of δ_{HOH} and libration mode (which is a combination of rocking, wagging and twisting motions) of water molecules. [53, 54] The IR spectra of Ca-crosslinked samples closely follow the trend of BBS-GC and/or neat alginate profiles (see red and blue curve for Alg-Ca-BBS(F) and Alg-Ca(F), respectively). As already reported by Larosa et al., [55] the influence of calcium is visible in the region of v_s(-OC=O) centered at about 1620 cm^{-1}: the shape of this peak is modified due to the change in cation density, radius and atomic weight when Ca^{2+} replaces Na^+. Also the region related to v(O-H) of Alg-Ca(F) sample is narrower than that of bare sodium alginate, likely due to the interaction of alginate hydroxyl and carboxylate groups with calcium ions and the consequent decrease in hydrogen bonds between OH groups. [55] The presence of BBS-GC is confirmed by the signal broadening at about 3400 cm^{-1}, due to the presence of -OH derived from both sodium alginate and BBS-GC and their reciprocal interactions.

Figure 2C displays the results of rheological measurements, giving information on Alg-Ca-BBS and Al-Ca hydrogels mechanical properties, namely the storage and loss moduli G' and G''. The gelation occurred in few seconds, as showed by the absence of a crossover point. G' was always higher than G" and both moduli did not change significantly over the frequency range analyzed, showing that both formulations behaved as viscous solids [56] throughout the whole test. G' and G'' for Alg-Ca(H) were higher than those found for Alg-Ca-BBS(H),

suggesting that the effect of BBS-GC macromolecules in the formation of the structure created by alginate chains and calcium ions is the increment of the mesh size of the gel network, as pointed out by our recent study. [22] Such enhanced spacing has been already found to be responsible of the storage modulus decrement in the case of polyvinyl alcohol-borax-polyethylenoxide hydrogels. [57]

Figure 2D shows the strain sweep when the frequency was fixed at 0.3 Hz. The critical strain, namely the point where the chains break, was extrapolated from the onset of G' curve slope change [58]: it was 2.4% for Alg-Ca(H) and 3.4% for Alg-Ca-BBS(H). This result implies that although G' for Alg-Ca-BBS(H) was lower than for Alg-Ca(H), BBS-GC globally stabilized the structure material. Possibly, the presence of BBS-GC forced the alginate chains to organize themselves in more tortuous paths, due to BBS-GC steric hindrance and hydrophobic interactions; this could explain the larger strain necessary to break the Alg-Ca-BBS gels, since the alginate chains required larger stresses to stretch themselves before rupturing. [59]

Overall, comparing rheological measurements of Ca-crosslinked samples with chitosan-based gels tested in our previous work, [22] we observed the improvement of mechanical features in presence of Ca^{2+} ions, since both G' and G'' values increased up to tenfold with respect to values obtained with chitosan. This effect is due to the Ca^{2+} action of tightly joining adjacent chains of alginate and BBS-GC molecules. [41]

Figure 3 shows the Field Emission Scanning Electron Microscopy (FE-SEM) images related to hydrogels and xerogels subjected to freeze-drying (also called cryogels). Xerogels are supposed to lose their structure due to evaporation at room temperature. On the contrary, cryogel cross-section images are more significant since the freeze-drying from the hydrated form is supposed to maintain the bulk network, as reported in the literature. [60]

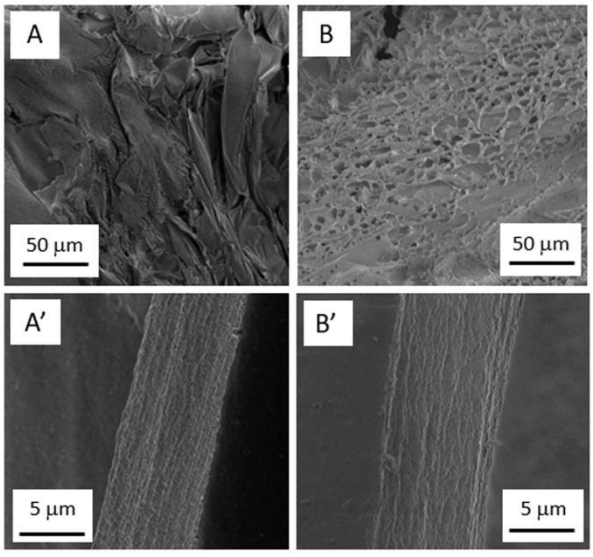

Figure 3. FE-SEM micrographs of cross-sections of cryogels (lyophilized) Alg-Ca(H) (image A) and Alg-Ca (F) (image A'), Alg-Ca-BBS(H) (image B) and Alg-Ca-BBS(F) (image B').

Both dried films are rather compact [61] and the morphology is not significantly modified by BBS-GC presence. On the contrary, the cross-section of the hydrogels after lyophilization appears very different: the bulky and amphiphilic BBS-GC molecules [62] induced the formation of large pores in the gel network, reflecting a different molecular organization among the gel chains already hypothesized from rheological measures.

Adsorption experiments

We used OII, CV and RH to evaluate the adsorption capacity of the different formulations. Figure S4 displays the curves of kinetic tests performed in the first hour of adsorption and Figure S5 reports the isotherms. All the isotherms (two of them, related to crystal violet adsorption on Alg-Ca-BBS(H) and Alg-Ca(H), are reported in Figure 4 as examples) were fitted by the Freundlich model (Eq. 1), known to describe non-ideal and reversible adsorption not restricted to the formation of monolayer, which reflects reasonably well the behaviors of the systems under study:

$$Log\ q_e = Log\ K_f + {}^{1}/_{n}\ LogC_e \qquad \text{(Eq.1)}$$

where q_e is the adsorbed dye concentration on the solid (µg g^{-1}), C_e is the equilibrium dye concentration (mg L^{-1}), and K_f and n are the Freundlich constants typical of the couple adsorbent/adsorbate at a given temperature. K_f relates to the adsorption capacity and 1/n represents the so-called adsorption intensity which is correlated to the energetics of the interaction adsorbent/adsorbate. [63]

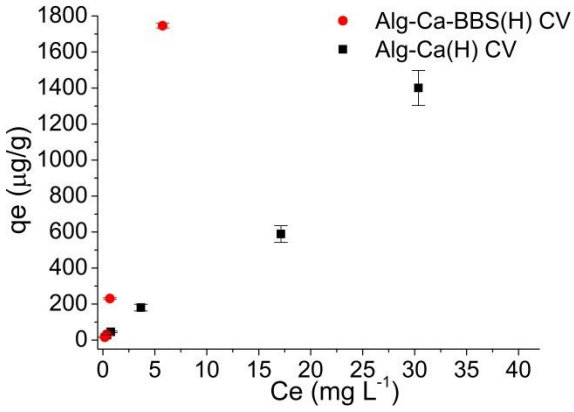

Figure 4. Adsorption isotherm related to adsorption of Alg-Ca-BBS and Alg-Ca hydrogels towards crystal violet; q_e is the adsorbed dye concentration on the solid (µg g^{-1}) and C_e is the equilibrium dye concentration (mg L^{-1}).

K_f data obtained by the Freundlich fitting are shown in Figure 5 and 1/n and R^2 values in Table S2. In most cases R^2 is close to 1 indicating that Freundlich model is adequate to describe the adsorption process.

Figure 5 shows that xerogels Alg-Ca(F) established negligible interactions with OII and RH. This can be explained by the compact structure of dried films, which disadvantaged the interaction with dyes. Alg-Ca(F) was effective only with CV (positively charged), thanks to its strong electrostatic interaction with negatively-charged alginate carboxylates. A similarly strong interaction with CV was found for all hydrogels and films (Figure 5, Figure S4, Figure S5).

Both hydrogels and films performed better -and similarly- when BBS-GC are introduced in the alginate network; these results confirm those previously obtained for alginate-chitosan PEC in 1-hour kinetic tests. [22] However, in that case chitosan further enhanced the adsorption percentage given its remarkable hygroscopy. The activity improvements caused by BBS-GC in all systems agree with previous reports that showed that BBS-GC dye adsorption is dependent not only on electrostatic attractions, but also on other kinds of less specific interactions - [3] as van der Waals and dispersion forces - [64] due to the BBS-GC complex structure constituted by hydrophilic functional groups, aromatic rings (bearing a π system) [6] and hydrophobic chains. This was verified also by the 1/n values (Table S2): both Alg-Ca(H) and Alg-Ca(F) showed 1/n values lower than 1, which indicate, when present, a homogeneous adsorption, [65] whereas in the presence of BBS-GC, 1/n values were always greater than 1, indicating a cooperative and more complex adsorption through multiple heterogeneous interactions. [63, 66]

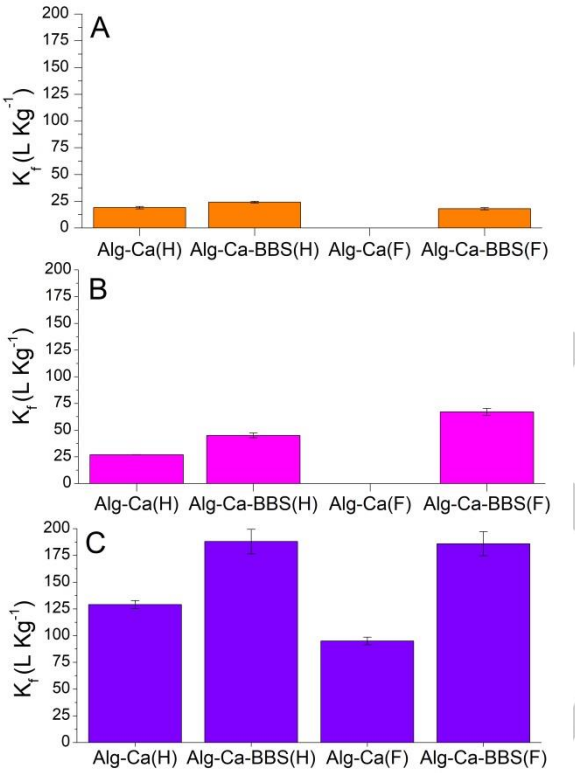

Figure 5. K_f values calculated from Freundlich model, related to adsorption of orange II (A), rhodamine B (B) and crystal violet (C).

Resuming the overall adsorption performances of BBS-GC-based gels, they were attributed to favorable electrostatic interaction between gel carboxylates and positively charged CV. The presence of the BBS-GC aromatic system and amino groups can be involved in the adsorption of OII (negatively charged and with an extended π system), whereas the adsorption of zwitterionic RH can be correlated to a combination of both the driving forces. Beyond the chemical aspect, BBS-GC caused some physical modification in the gel, in particular opening the network and creating a certain macroporosity, that can better accommodate the adsorbates, with respect to bare alginate gels used as references.

With respect to literature data, the materials under study cannot equal the important performance obtainable by complex systems, whose behaviors are optimized by several synthetic steps (see Table S3 for some comparison on CV capture), but these materials represent good systems as for simplicity of preparation, easiness of storage and reuse of organic refuses employed in their preparation. Moreover, their specific affinity towards positively charged substrates opens the way to the selective capture of cationic molecules.

Conclusion

We successfully incorporated biowaste-derived substances (BBS-GC) to alginate-based hydrogels and xerogels crosslinked with calcium ions to increase efficiency as contaminant adsorbents for water remediation. We assessed the formation of easy-to-form and stable gels, as witnessed by the rheological and swelling tests performed. The presence of BBS-GC modified the final physicochemical properties evaluated by a multi-analytical approach, in terms of vibrational features, increment of the mesh size within the 3D network and development of hydrogel macroporosity.

We adopted the prepared gels as adsorbents towards different dyes often found in industrial effluents, namely orange II (negatively charged), rhodamine B (zwitterionic) and crystal violet (positively charged) and, for the first time, we studied the adsorption mechanism. In all cases, the BBS-GC-containing samples performed best, thanks to the multiple and heterogeneous interactions established between BBS-GC and the dyes. BBS-GC-containing xerogels demonstrated to reach comparable adsorption levels with respect to hydrogels, and, thus, to be additionally advantageous because xerogels do not require any condition to maintain the hydration state and can be easily stored. While these gels were able to adsorb less dye than chitosan-BBS-GC-alginate gels previously tested in our group, the use of Ca^{2+} instead of chitosan simplified the preparation procedure and improved the gels mechanical properties.

These results show that it is possible to add value to marine-derived polymers and biowaste-derived substances as they become environmentally-friend and low-cost chemicals for high level sustainable technological applications. The concept of “waste cleaning waste” well fits this study as the prepared gels showed high efficiency in the removal of charged dyes from model solutions. The efficiency of the materials in real wastewater treatment will be tested in the future to evaluate effects and possible interferences of components normally present in water.

Experimental Section

Materials Sodium alginate (CAS 9005-38-3), $CaCl_2$ (anhydrous, ≥93%, CAS 10043-52-4) as well as the dyes orange II (sodium salt, >85%, CAS 633-96-5), crystal violet (>90%, CAS 548-62-9), rhodamine B (>95%, CAS 81-88-9) were purchased from Sigma Aldrich.

The Bio-Based Substances isolated from Green Compost (BBS-GC) were obtained following a previously developed procedure. [67]

We prepared all the aqueous solutions using MilliQ™ water and we used all the reagents without further purification.

Synthesis of the gels and stability test We put the sodium alginate solution (2 wt.% in water) either in an open glass vial (28×57 mm) or in a glass Petri dish (60×15 mm) and mixed with the BBS-GC aqueous solution (2 wt.%). Subsequently, we added the crosslinker solution of calcium chloride (5 wt.% in water) at a volume ratio of alginate: $CaCl_2$: BBS-GC = 2:1:1. We left the precursors to interact for about 30 minutes, despite the gelation occurred in few seconds (indeed, the gelation point was neither acquirable by rheological measurements as discussed before). The process led to the formation of a soft disc with the same size as the container used.

After crosslinking, we added 10 mL of MilliQ™ water to the samples which were, then, gently shaken in a rotating apparatus for 10 minutes (10 rpm). The procedure was repeated ten times per sample, using fresh water at every cycle. After each rinsing cycle, the supernatant was separated for analyzing the amount of excess chlorides through ion chromatography technique to assess cleaning effectiveness and the eventual BBS-GC release via UV-Vis spectroscopy, following the absorption at 280 nm. For ion chromatography analysis, we used a Dionex DX500 instrument equipped with Anion Self-Regenerating Suppressor-Ultra (ARSR-ULTRA, 4 mm, Dionex), a conductimeter detector (ED 40, Dionex) and a GP40 pump (Dionex). We injected 20 µL into the AS9-HC column Dionex Ion Pack (250 mm × 4 mm i.d.) with isocratic conditions: 100% of K_2CO_3 9 mM (flow = 1.0 mL min^{-1}), in these conditions the chloride retention time was *ca.* 6 min. For spectroscopic analyses, we used a double-beam UV-visible spectrophotometer CARY 100 SCAN-VARIAN and a quartz cell with 1 cm path length.

After rinsing, we kept the gels prepared in the vials hydrated by sealing the containers, whereas we put those formed in Petri dishes in a fume hood overnight at room temperature (RT, about 25°C) to allow the evaporation of water, thus obtaining dried films (xerogels). We also produced hydrogels and films without BBS-GC as control samples, with volume ratio of alginate:$CaCl_2$ = 2:1.

Physicochemical characterization We evaluated the swelling of dried films: they were soaked in water, periodically removed (6 times along 6 hours), gently compressed with a paper filter to remove the excess of moisture and weighed at RT before returning them to the water bath. [68] The swelling ratio (S) was calculated according to Eq. 2:

$$S = W_t/W_0 \qquad \text{(Eq. 2)}$$

where W_t indicates the mass at each time, whereas W_0 corresponds to the initial dry mass.

We performed thermogravimetric analysis (TGA) using a TGA Q600 (TA Instruments), with an open alumina sample holder, under nitrogen flow and a heating ramp of 10°C min^{-1} from 30 to 800°C. We carried out the measurements on fragments of dried films (approximately 10 mg) as well as sodium alginate and BBS-GC. We also analyzed the thermal profiles of the hydrogels to assess the amount of water entrapped in the 3-D networks, studying the range 30-200°C.

We recorded Fourier transform infrared (FT-IR) spectra on a Bruker Vector 22 spectrophotometer equipped with a Globar source and DTGS detector, in the 4000-400 cm^{-1} range, with 128 scans and resolution 4 cm^{-1}. The instrument collected spectra of dried gels, whereas for the spectra of reference alginate and BBS-GC, we dispersed the related powders in KBr (1:20 weight ratio). Hydrogels were not analyzed by this technique due to the prevailing content of water whose spectroscopic signals cover a very large part of the spectrum.

We performed rheological measures on *ad hoc* samples of 9 x 4 mm to determine the conservative and dissipative moduli (G' and G'') using a rotational rheometer DISCOVERY HR1 (TA Instruments) equipped with Peltier plate temperature control. The geometry used was the parallel plate, with knurled surface to prevent sliding of the samples (diameter=20 mm) and the gap was set at 500 µm. Frequency sweep analyses were performed in the linear viscoelastic region (LVR) from 0.1 to 50 Hz, γ= 1%, as established by initial stress sweep tests.

We carried out Field Emission Scanning Electron Microscopy (FE-SEM) analysis on freeze-dried hydrogels (also called cryogels in the text, obtained by the lyophilizer BenchTop K freeze dryer; VirTis, SP Industries) and dried films using a FEI Inspect F-50 equipped with detectors for secondary electrons collection. Cross-sections the samples were observed at an acceleration voltage of 1 kV.

Adsorption tests We tested the adsorption ability of a single gel disc in the form of hydrogel or dried film towards 5 mL of different aqueous dye solutions at 22.0±0.5°C and at constant pH of 6.5 (naturally obtained by soaking the gels in dye solutions). We performed adsorption trials on solutions of orange II (OII), crystal violet (CV) and rhodamine B (RH), whose molecular structures are reported in Figure S2. Once determined in preliminary tests the minimum time to reach the adsorption equilibrium (4 hours), we obtained the adsorption isotherms using dye concentrations in the range 0.5-40 mg L^{-1} by measuring the intensity variations of the signals at 485 nm for OII, 590 nm for CV and 555 nm for RH by means of an UV-visible spectrophotometer (CARY 100 SCAN-VARIAN equipped with a quartz cell with 1 cm path length).

Acknowledgements

This work was realized with the financial support for academic interchange by the Marie Sklodowska-Curie Research and Innovation Staff Exchange project funded by the European Commission H2020-MSCA-RISE-2014 within the framework of the research project Mat4treaT (Project number: 645551) and the Canada Research Chair program. Compagnia di San Paolo and University of Torino are gratefully acknowledged for funding Project Torino_call2014_L2_126 through "Bando per il finanziamento di progetti di ricerca di Ateneo – anno 2014" (Project acronym: Microbusters) and for "Bando per il finanziamento ex-post di progetti di ricerca di Ateneo – anno 2018". Additionally, authors would like to acknowledge Dr. Maria Carmen Valsania and Dr. F. Cesano (University of Torino, Italy) for their precious collaboration.

Keywords: Gels • Biowaste-derived substances • Alginate • Adsorption • Water treatments

[1] United Nations, Department of Public Information Sustainable Development Goals for People and Planet: Sustainable Development Knowledge Platform. Available online: https://sustainabledevelopment.un.org/post2015/transformingourworld (accessed on 07 april 2020).

[2] W. Ouyang, T. Chen, Y. Shi, L. Tong, Y. Chen, W. Wang, J. Yang, J. Xue, *Water Environ. Res*. **2019**, *91*, 1350-1377.

[3] M. L. Tummino, M. L. Testa, M. Malandrino, R. Gamberini, A. Bianco Prevot, G. Magnacca, E. Laurenti, *Nanomaterials* **2019**, *9*, 162.

[4] M. Bellucci, F. Marazzi, L. S. Naddeo, F. Piergiacomo, L. Beneduce, E. Ficara, V. Mezzanotte, *J. Chem. Technol. Biotechnol*. **2020**, *95*, 959-966.

[5] G. Z. Kyzas, M. Kostoglou, *Materials* ***2014***, *7*, 333-364.
[6] R. Nisticò, F. Cesano, F. Franzoso, G. Magnacca, D. Scarano, I. G. Funes, L. Carlos, M. E. Parolo, *Chemosphere* **2018**, *202*, 686-693.
[7] V.K. Gupta, Suhas, *J. Environ. Manage*. **2009**, *90*(8), 2313-2342.
[8] S. De Gisi, G. Lofrano, M. Grassi, M. Notarnicola, *Sustainable Mater. Technol.* **2016**, *9*, 10-40.
[9] G. Chen, K. J. Shah, L. Shi, P.-C. Chiang, *Appl. Surf. Sci.* **2017,** *409*, 296-305.
[10] R. Sule, A. K. Mishra, *Appl. Sci.* **2019**, *9*, 4407..
[11] Y. Cui, Z. He, Y. Xu, Y. Su, L. Ding, Y. Li, *Chem. Eng. J.* **2021**, *405,* 126608.
[12] X. Dong, Y. Lin, Y. Ma, L. Zhao, *Inorg. Chim. Acta* ***2020****, 510*, 119748.
[13] H. A.El-saied, E. A. Motawea, *J. Polym. Environ*. **2020** *28*, 2335–2351.
[14] R. Soltani, A. Marjani, R. Soltani, S. Shirazian, ., *Sci. Rep*. **2020** *10*, 9788.
[15] M. C. Pazos, L. Ruiz Bravo, S. E. Ramos, F. J. Osuna, E. Pavón, M. D. Alba, . *Appl. Clay Sci.* **2020***. 196*, 105749.
[16] H. Liu, P. Li, F. Qiu, T. Zhang, J. Xu, *Food Bioprod. Process* **2020***, 123*, 177–187.
[17] P. Stathi, Y. Deligiannakis, *J. Colloid Interface Sci.* **2010**, *351*(1), 239-247.
[18] N.B. Singh, G. Nagpal, S. Agrawal, Rachna, *Environ. Technol. Innov.* **2018**, *11*, 187-240.
[19] Renu, M. Agarwal, K. Singh, *J. Water Reuse Desalin.* **2017**, *7*(4), 387-419.
[20] C. Ouwerx, N. Velings, M.M. Mestdagh, M.A.V. Axelos, *Polym. Gels Netw*. **1998**, *6*(5), 393-408.
[21] F. Guerretta, G. Magnacca, F. Franzoso, P. Ivanchenko, R. Nisticò, *Mater. Lett.* **2019**, *234*, 339-342.
[22] M. L. Tummino, G. Magnacca, D. Cimino, E. Laurenti, R. Nisticò, *Int. J. Mol. Sci.* **2020**, *21*(2), 550.
[23] B. Sarker, A. R. Boccaccini, in Alginates and Their Biomedical Applications (Eds.: B.H.A. Rehm, M.F. Moradali), Springer Singapore, Singapore, **2018**, pp. 121–155.
[24] S. H. Ching, N. Bansal, B. Bhandari, *Crit. Rev. Food Sci. Nutr.* **2017,** *57*(6), 1133-1152.
[25] N. Shaari, S.K. Kamarudin, *J. Power Sources* **2015,** *289*, 71-80.
[26] P. Bosch-Roig, G. Lustrato, E. Zanardini, G. Ranalli, *Ann. Microbiol*. **2015**, *65*, 1227-1241.
[27] S. Thakur, B. Sharma, A. Verma, J. Chaudhary, S. Tamulevicius, V. K. Thakur, *J. Cleaner Prod.* **2018**, *198,* 143-159.
[28] H. M. C. Azeredo, K. W. Waldron, *Trends Food Sci. Technol.* **2016,** *52*, 109-122.
[29] S. Asadi, S. Eris, S. Azizian, *ACS Omega* **2018**, *3*(11), 15140-15148.
[30] Y. Vijaya, S. R. Popuri, A. S. Reddy, A. Krishnaiah, *J. Appl. Polym. Sci.* **2011**, *120*, 3443-3452.
[31] O. Bunkoed, P. Kanatharana, *Microchim. Acta* **2015**, *182*, 1519-1526.
[32] W. S. Wan Ngah, L. C. Teong, M. A. K. M. Hanafiah, *Carbohydr. Polym.* **2011**, *83*, 1446-1456.
[33] F. Franzoso, R. Nisticò, F. Cesano, I. Corazzari, F. Turci, D. Scarano, A. Bianco Prevot, G. Magnacca, L. Carlos, D. O. Martire, *Chem. Eng. J.* **2017,** *310*, 307-316.
[34] R. Sadraei, M.C. Paganini, P. Calza, G. Magnacca, *Nanomaterials* **2019**, *9*(5), 731.
[35] P. Avetta, F. Bella, A. Bianco Prevot, E. Laurenti, E. Montoneri, A. Arques, L. Carlos, *ACS Sustain. Chem. Eng.* **2013**, *1*, 1545–1550.
[36] Independent Commodity Intelligence Services Siteweb, https://www.icis.com/explore/resources/news/2002/11/15/185117/producers-seek-price-increases-in-the-mature-alginates-market/#:~:text=Food%2Dgrade%20salts%20of%20alginate,%244.50%20per%20pound%20last%20year
[37] K.Y. Lee, D.J. Mooney, *Prog. Polym. Sci*. **2012**, *37*, 106-126.
[38] http://publications.iowa.gov/20047/
[39] R. Nisticò, *Resources* **2017**, *6*, 65.
[40] R. Nisticò, P. Evon, L. Labonne, G. Vaca-Medina, E. Montoneri, M. Francavilla, C. Vaca-Garcia, G. Magnacca, F. Franzoso, M. Negre, *ChemistrySelect* **2016**, *1*, 2354-2366.
[41] G. Lawrie, I. Keen, B. Drew, A. Chandler-Temple, L. Rintoul, P. Fredericks, L. Grøndahl, *Biomacromolecules* **2007**, *8*(8), 2533-2541.
[42] C. R. Holkar, A. J. Jadhav, D. V. Pinjari, N. M. Mahamuni, A. B. Pandit, *J. Environ. Manage.* **2016**, *182*, 351-366.
[43] B. Lellis, C. Z. Favaro-Polonio, J. A. Pamphile, J. C. Polonio, *Biotechnol. Res. Innov.* **2019**, *3*(2), 275-290.
[44] D. A. Yaseen, M. Scholz, *Int. J. Environ. Sci. Technol.* **2019**, *16*, 1193–1226.
[45] N. Chubar, *J. Colloid Interface Sci*. **2011**, *357*(1), 198–209.
[46] J. Kopeček, *Nature* **2002,** *417,* 389-391.
[47] C. Qiao, X. Ma, J. Zhang, J. Yao, *Carbohydr. Polym*. **2019,** *206*, 602–608.
[48] P. Laurienzo, M. Malinconico, A. Motta, A. Vicinanza, *Carbohydr. Polym*. **2005,** *62*(3), 274-282.
[49] J. P. Soares, J. E. Santos, G. O. Chierice, E. T. G. Cavalheiro, *Ecletica Quim*. **2004**, *29*(2), 57-64.
[50] A. Konwar, D. Chowdhury, *RSC Adv.* **2015**, *5*, 62864-62870.
[51] F. O. M. S. Abreu, C. Bianchini, M. M. C. Forte, T. B. L. Kist, *Carbohydr. Polym*. **2008**, *74*, 283-289.
[52] C. Sartori, D. S. Finch, B. Ralph, K. Gilding, *Polymer* **1997,** *38*(1), 43-51.
[53] J.-J. Maxa, C. Chapados, *J. Chem. Phys.* **2009**, *131*, 184505.
[54] https://webbook.nist.gov/cgi/cbook.cgi?ID=C7732185&Type=IR-SPEC&Index=1
[55] C. Larosa, M. Salerno, J. Silva de Lima, R. Merijs Meri, M. Fernandes da Silva, L. Bezerra de Carvalho, A. Converti, *Int. J. Biol. Macromol.* **2018,** *115*, 900-906.
[56] K. Almdal, J. Dyre, S. Hvidt, O. Kramer, *Polym. Gels Networks* **1993**, *1*(1), 5-17.
[57] C. Riedo, F. Caldera, T. Poli, O. Chiantore, *Heritage Sci.* **2015,** *3,* 23.
[58] A. E. Horvath, T. Lindström, *J. Colloid Interface Sci.* **2007,** *309*(2), 511-517.
[59] M. A. Faers, P. F. Luckham, *Langmuir* **1997**, *13*(11), 2922-2931.
[60] H. Qu, S. Bhattacharyya, P. Ducheyne, Sol–Gel Processed Oxide Controlled Release Materials, in Comprehensive Biomaterials II, Elsevier, **2017**, 617-643.
[61] M. Alam, S. A. Mirbagheri, M. R. Ghaani, *Heliyon* **2019**, *5*(2), e01196.
[62] F. Deganello, M. L. Tummino, C. Calabrese, M. L. Testa, P. Avetta, D. Fabbri, A. Bianco Prevot, E. Montoneri, G. Magnacca, *New J. Chem.* **2015**, *39*, 877–885.
[63] M. Islam, P. C. Mishra, R. Patel, *Chem. Eng. J.* **2013,** *230*, 48-58.
[64] E. D. Mordvinova, M. V. Parkhats, Y. Chen, I. P. Pozdnyakov, *Mendeleev Commun.* **2019**, *29*(4), 426-428.
[65] S. V. Mohan, J. Karthikeyan, *Environ. Pollut.* **1997,** *97*(1-2), 183-187.
[66] S. Liu, *J. Colloid Interface Sci.* **2015,** *450*, 224-238.
[67] D. Palma, A. Bianco Prevot, L. Celi, M. Martin, D. Fabbri, G. Magnacca, M.R. Chierotti, R. Nisticò, *Catalysts* **2018**, *8*(5), 197.
[68] R. You, C. Xiao, L. Zhang, Y. Dong, *Int. J. Biol. Macromol.* **2015,** *79*, 498–503.

Entry for the Table of Contents

Insert graphic for Table of Contents here. ((Please ensure your graphic is in **one** of following formats))

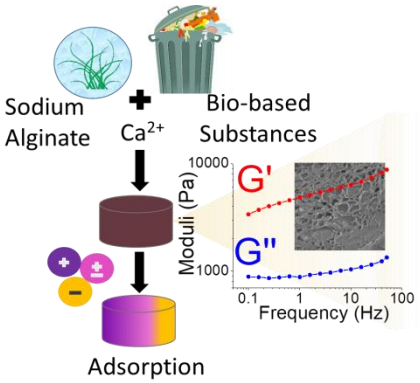

Substances extracted from composted biowaste (BBS-GC) were combined with sodium alginate and crosslinked with Ca^{2+}, to prepare hydrogels and dried films through an easy and green procedure. BBS-GC addition in the 3D network gave peculiar physico-chemical properties to samples and enhanced their adsorption capability towards dye solutions as model water contaminants.